Powder Technology 269 (2015) 101–109

Contents lists available at ScienceDirect

Powder Technology

journal homepage: www.elsevier.com/locate/powtec

Dynamical effects in the segregation of granular mixtures in quasi 2D piles

D. Rodríguez [a], J.G. Benito [c], I. Ippolito [a], J.-P. Hulin [b,*], A.M. Vidales [c], R.O. Uñac [c]

[a] Grupo de Medios Porosos, Facultad de Ingeniería, Universidad de Buenos-Aires, Paseo Colón 850, 1063 Buenos Aires, Argentina
[b] Univ Paris-Sud, CNRS, F-91405. Lab FAST, Bât 502, Campus Univ, Orsay F-91405, France
[c] INFAP-CONICET, Departamento de Física, Facultad de Ciencias Físico Matemáticas y Naturales, Universidad Nacional de San Luis, Ejército de los Andes 950, D5700HHW San Luis, Argentina

ARTICLE INFO

Article history:
Received 14 May 2014
Received in revised form 27 August 2014
Accepted 1 September 2014
Available online 8 September 2014

Keywords:
Granular
Mixing
Segregation
Layering
Spatiotemporal

ABSTRACT

The dynamics of segregation, mixing and layering is studied during the build-up of quasi-2D piles of two different species of grains of different diameters (*i.e.* 1 mm glass beads and either 3 mm glass beads or 3.1 mm coriander seeds). The ranges of existence of the different flow regimes are studied as a function of the relative volume flow rates of the two species and of the drop height; the variation of the mean slope of the pile with time is shown to depend on the flow regime. Complete segregation occurs when the larger grains are coriander seeds while there is always some mixing for glass beads, although the ratio between the sizes of the particles is the same in both cases. A layered regime is observed for glass beads of same geometry (*i.e.* spheres) and density but of two different diameters: it is accompanied by variations of large amplitude of the slope of the pile. No layering occurs when the large particles are coriander seeds instead of glass beads. The local processes underlying these regimes are analyzed quantitatively from spatiotemporal diagrams of the profile of the free surface and the characteristic velocities of the different types of displacements of the grains are determined. Avalanches are only observed for glass beads and in the layered regime and play an important part in the development of the layers.

1. Introduction

The build-up of granular piles from flows of grains poured from above and/or flowing on a slope is a particularly important and widespread process in nature and in civil or food engineering. A particularly important issue is the occurrence of segregation and/or layering when the pile is built up from grains of different geometries or sizes. Several authors have reported, for instance, a complete separation of the different grain species or the spontaneous appearance of alternate strata of each of them [1–9]. Several mechanisms may account for these observations: they generally associate the effects of the differences in the size and the geometry (smooth or rough, rounded or angular) of the different types of grains.

In a previous paper [10], we showed that such a stratification may also be observed in mixtures of grains of different sizes but with the same geometry (spherical beads) and made of the same material (glass). In this latter work, we studied the different spatial distributions of the two different types of grains (mixing, segregation, stratification) as a function of their flow rates and of the lateral displacement of the injection point (industrial processes frequently involve such displacements). We also presented a method for characterizing quantitatively the distribution of the grains.

The present work is devoted to the quantitative analysis of the dynamics of mixing and segregation for similar mixtures of grains of different sizes. This analysis is performed both at the global scale from the variation with time of the mean slope of the surface of the pile and of the angles of repose and of maximum stability and, at the local scale, from the velocities of individual or groups of grains obtained from spatiotemporal diagrams. Moreover, we compare results obtained by using either glass beads or coriander seeds as the larger grains: while the two species have a similar global shape (spherical) and diameter (3 and 3.1 mm), the coriander seeds are rougher and less dense. This allows us to study the influence of different roughness and densities on layering or segregation.

Like those reported in Ref. [10] and like many others dealing with layering, the present measurements are performed in a quasi-2D cell of small gap. This allows us first to obtain the quantitative information of interest to us by non-invasive photo or video techniques using grains of different colors. This configuration allows one indeed to observe simultaneously the inside and the surface of the pile: it would be difficult to even identify with certainty either stratification or segregation if only the surface was visible. Moreover, it was observed that the amplitude of the layered pattern could increase with the ratio d/e of the diameter d of the largest grains and the gap e between the cell walls [20]: at low values of d/e, a motion of the grains transverse to the mean flow may take place and account for reduced layering. A dependence of layering on d/e was also reported in Ref. [7]. The influence of d/e on the slope

* Corresponding author. Tel./fax: +33 169158062/60
E-mail address: hulin@fast.u-psud.fr (J.-P. Hulin).

http://dx.doi.org/10.1016/j.powtec.2014.09.001
0032-5910/

of the surface and on the degree of segregation for values similar to those used in the present experiments seems, in contrast to be low [19].

In this paper, we analyze first the variation with time of the mean slope of the piles in the different regimes (mixing, segregation and stratification). We discuss then spatiotemporal diagrams of the profile of the surface of piles built-up by the downflow of a homogenous mixture of two types of grains. These diagrams allowed us to follow the motion of individual grains or groups of grains and to investigate at the local scale the mixing/segregation/layering processes. Finally, the influence of the roughness and density of the grains is analyzed by comparing the results obtained using either glass beads with a smooth surface or rough coriander seeds (used in the food industry) as the large grains (the smaller grains are glass beads in both cases).

2. Experimental setup and procedure

A schematic view of the experimental setup is displayed in Fig. 1. The grain piles build up inside a quasi two-dimensional transparent parallelepipedic Plexiglas cell *C* (width: 400 m, height: 150 mm cell gap: $e = 10$ mm). The two species of grains flow separately from two vibrating feeders *F* with adjustable flow rates into a funnel followed by a mixing channel (3*DM*) of square section (21×21 mm) containing a series of 8 grids made of copper wires with square apertures of sides 7 mm; each grid is shifted by half a mesh size from the previous one so as to ensure better mixing. This system mixes the grains by a diffusion mechanism described in Refs. [11,12]: the grains experience indeed random motions in the horizontal plane due to their collisions with the wires. After a wedge shaped transition the grains move into a second device (2*DM*) with a rectangular section (32×5 mm) acting as a 2*D* mixer and a distributor. Here, mixing is induced by a triangular network of obstacles of height also equal to 5 mm: these obstacles reduce the velocity of the grains before they flow into the cell through a 16 mm wide constriction. The reduced transverse size of this section allows one to insert it into the cell. Independent experiments have been performed with the different types of beads/grains in order to determine the ranges of flow rates for which no obstruction took place: all the experiments reported here have been performed for values corresponding to stationary continuous flows.

The mass flow rates of the different types of grains provided by the vibrating feeders varied (from separate measurements) from 0.1 to 0.4 $g \cdot s^{-1}$ for glass beads and from 0.05 to 0.24 $g \cdot s^{-1}$ for coriander. For the actual experiments, the ratio of the time averaged mass flow rates of the two species is determined by weighing the masses of each species present in the cell after a given time lapse. This ratio is directly equal to the ratio *q* of the volume flow rates for experiments using only glass beads; for those using small glass beads and coriander grains, the ratio of the masses must be divided by that of the densities.

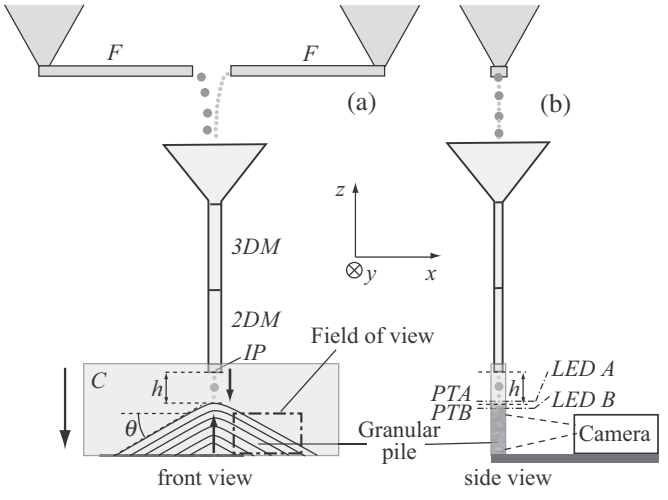

Fig. 1. (a) Schematic front view of the experimental setup: *F*: feeders, *3DM*: mixer, *2DM*: 2D mixer, *IP*: injection point, *C*: cell, *h*: distance between the outlet of the mixer sand the top of the pile. (b) Side view and devices keeping the drop height *h* constant: *PT*: photodetectors, *LED*: light emitting diodes.

The kinetic energy E_c of the grains influences significantly their final distribution: the grains are slowed down inside the mixers so that their energy is mostly acquired along the vertical path of height *h* between the outlet *IP* and the top of the pile. In order to keep *h* (and, therefore, E_c) constant with time, the feeders and the mixers remain fixed while a servo control system moves the cell vertically: it keeps the top of the pile between two fixed *IR* detectors *PTA* and *PTB* spaced vertically by 5 mm. This distance is larger than the size of the largest grains used in the experiments (*i.e.* ~3 mm) so that a single grain cannot activate the two detectors at the same time.

The influence of the kinetic energy E_c of the impacting grains is studied by comparing experiments using the same grains but different values of *h* equal to 10, 30 and 50 mm. These distances are too small to reach the terminal velocities of the grains: for the present beads/grains, the latter would indeed range from the 6 to 14 $m \cdot s^{-1}$ and would be reached above distances ranging from 2 to 10 m (these values are obtained using classical expressions from the literature for the drag coefficients). Due to the low velocity of the grains at the outlet of the distributor–mixers, their impact velocity will be of the order of $\sqrt{2gh}$ and range between 0.45 and 1 $m \cdot s^{-1}$.

The grains used in this work were spherical glass beads of average diameter $d = 1$ mm and either larger ($d = 3$ mm) glass beads or globally spherical coriander seeds with a rough surface and $d = 3.1$ mm. The values of the diameters *d* and densities [13] ρ_g of the different types of beads/grains are listed in Table 1 together with their standard deviations. In order to make them visible and to identify them, the glass beads are painted using an alcohol soluble dye (red for the larger beads and blue for the smaller ones). The dye does not modify significantly the surface of the beads and, therefore, their mechanical properties. An important parameter in these phenomena is the restitution coefficient C_r for the energy of colliding grains. This coefficient has been measured through independent experiments in which a grain (or bead) of one species hits another of the same species glued onto a solid horizontal surface. The values of C_r obtained in this way for 3 mm glass beads and 3.1 mm coriander grains are listed in Table 1: in spite of the different properties of the coriander grains and glass beads, the values of the corresponding restitution coefficients are remarkably similar.

In the present experiments, both the influence of the drop height *h* of the grains and that of the ratio *q* between the volume flow rates of the two sizes of grains are investigated. The ratio *q* is given by:

$$q = \frac{m_1}{m_2}\,\frac{\rho_2}{\rho_1} \tag{1}$$

in which m_i and ρ_i are the mass flow rate and density of species *i* with $i = 1$ for the grains of larger diameter and $i = 2$ for those of smaller

Table 1
Mean values and standard deviations of the diameter, density, and restitution coefficient for the three species of beads/grains used in the experiments and of the angle of repose θ_R and the maximum angle of stability θ_M of piles built from these species ($h = 30$ mm). In the text, the angles corresponding to 3 and 1 mm glass beads are respectively referred to as θ_{R1} (θ_{M1}) and θ_{R2} (θ_{M2}).

Species	*d* (mm)	ρ_g $10^3 \times kg/m^3$	C_r	θ_R (°)	θ_M (°)
Glass beads	1 ± 0.15	2.55 ± 0.05		29 ± 0.5	32 ± 0.5
Glass beads	3 ± 0.25	2.55 ± 0.05	0.85 ± 0.02	28 ± 0.1	29 ± 0.1
Coriander Grains	3.1 ± 0.25	0.6 ± 0.06	0.84 ± 0.03	31 ± 0.4	34 ± 0.5

diameter. The ratio m_i/ρ_i represents the volume of the grains of type i (excluding voids) falling on the pile per unit time.

Two types of measurements are performed during these experiments. The first one is the spatial distribution of the different types of grains in the pile at the end of the build-up process: it is determined on images provided by a Nikon D70S digital camera (picture size: 3008×2000 pixels). The analysis of these images allows one to identify the corresponding regime (mixing, segregation or layering).

The second type of measurement analyzes the dynamical characteristics of the build-up of the piles. This is achieved by means of video recordings obtained using a Casio Exilim FH25 camera (frame size: 1280×720 pixels) with a rate of 30 fps (each pixel corresponds to a square of 0.125×0.125 mm on the object and the field of view covers only a part of the pile (see Fig. 1a)). In this latter case, the camera follows the vertical motion of the cell so as to remain fixed with respect to it: this makes it possible to detect the motion of individual or small groups of grains at the surface of the pile. For that purpose, each frame recorded by the camera is processed by means of MATLAB™ subroutines. A first step is the precise determination of the profile of the free surface of the pile. For this, the image is cleaned up in order to eliminate the noise due to the CCD transducer as well as clear shades near the center of the beads due to reflections. A thresholding algorithm is then applied to the color image so that the pile corresponds to a black region and the other parts of the experiment to a white one: the profile $z(x, t)$ of the surface of the pile at a time t corresponds then to the boundary of the black region (x is the horizontal distance parallel to the width of the cell in Fig. 1) and $z(x)$ is the corresponding vertical coordinate of the surface.

A first interesting quantitative feature of these profiles is the time dependence of the angle θ of the surface with the horizontal which provides information on the large scale evolution of the geometry of the pile. The mean slope $tan\theta$ is determined by a linear regression over the variation $z(x)$ at the time of interest. The range of x values over which the measurement is performed does not include the rounded top of the pile nor its bottom where, frequently, large beads gather and form a bulge. In some flow regimes (see Fig. 3 below), the two types of beads get macroscopically segregated: the local slope may then vary significantly along the surface. However, the fluctuations of the local angle are too large to define a different angle for different parts of the pile: we report therefore mean values of the angle θ determined by a regression on the whole surface profile (excluding, as mentioned above, the top and bottom of the pile.)

More local changes of the profile corresponding to the motion of individual grains or small groups of grains are detected by means of spatiotemporal diagrams: these are grayscale images in which the vertical coordinate corresponds to time and the horizontal one to the distance x. For a given line corresponding to the time t, the gray level at point x corresponds to the difference $\Delta z(x, t) = z(x, t + \delta t) - z(x, t)$ in which $\delta t = 1/30$ s is the time interval between two frames. The points of the surface where the level $z(x)$ has changed between times t and $t + \delta t$ due to the motion of one or several grains appear therefore with different gray levels on the diagram. On these diagrams, white corresponds to $\Delta z = 2$ mm (or more) and black to $\Delta z = -2$ mm: these are typical variations of the local height of the surface produced by the arrival (or departure) of a large grain of diameter ~ 3 mm. One should note that the objective of these diagrams is not however to map precisely the variations of the local height of the surface; it is to provide a sensitive detection of the motions of individual or groups of large grains at the surface of the pile and to allow for the determination of their instantaneous velocities.

3. Experimental results

3.1. Time dependence of the slopes of piles of a single species of grains

A necessary first characterization is the comparison of the angles of repose and of maximum stability for packings using a single species of grains: this is achieved by measuring the changes with time of angle θ of piles of one of these species. These curves represent a reference for comparisons with similar variations observed for binary mixtures.

Fig. 2a–c compares the variations obtained for drop heights $h = 10$, 30 and 50 mm, respectively for 1 and 3 mm glass beads and 3.1 mm coriander grains. We assume that the values of the angle of repose θ_R and the maximum angle of stability θ_M are respectively those at which the motion of the grains stops after one or several avalanches and restarts when a new one occurs. The experimental values of θ_R and θ_M obtained in this way and averaged over 3 different experiments performed with the same control parameters are listed in Table 1.

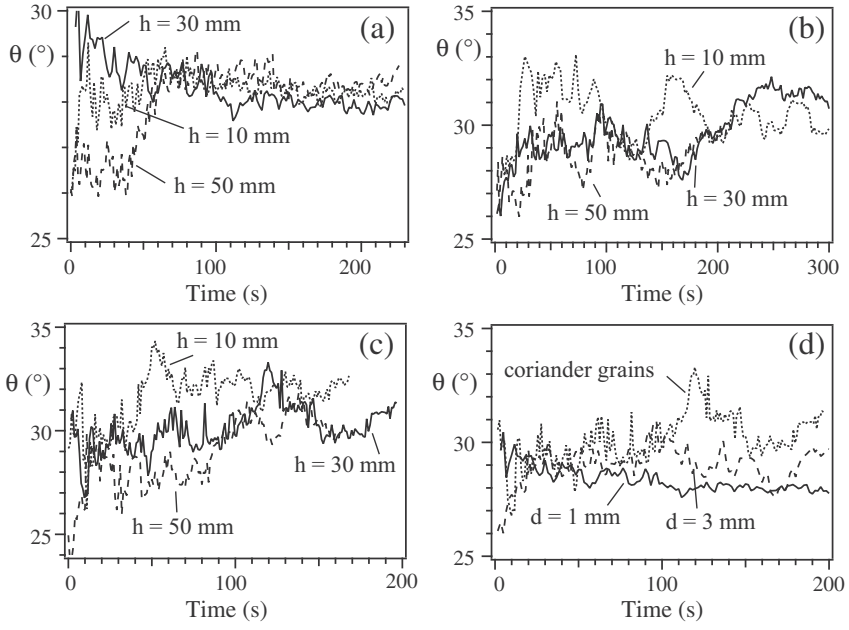

Fig. 2. Time dependence of the mean angle θ of the surface of the pile from the horizontal during experiments using only one grain species. Glass beads with (a) $d = 1$ mm and (b) $d = 3$ mm, (c) coriander grains with $d = 3.1$ mm: $h = 10$ mm (dotted), $h = 30$ mm (continuous), $h = 50$ mm (dashed). (d) Constant drop height $h = 30$ mm: glass beads with $d = 3$ mm (dashed line) and $d = 1$ mm (continuous); coriander grains: $d = 3.1$ mm (dotted). Time interval between data points on the curves = 1 s (30 frames).

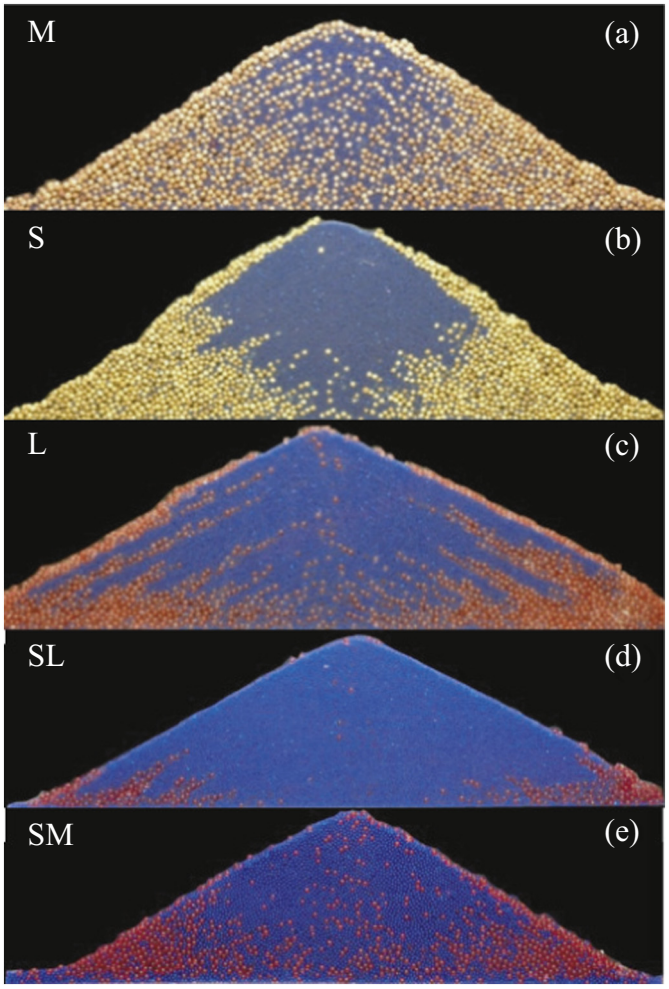

Fig. 3. Grain distributions for different flow rate ratios q, falling distances h and grain materials. (a), (b) $d_1 = 3.1$ mm (coriander), $d_2 = 1$ mm (glass) – (a) $q = 2$, $h = 50$ mm; (b) $q = 0.8$, $h = 10$ mm. (c), (d), (e): $d_1 = 3$ mm (glass), $d_2 = 1$ mm (glass), – (c) $q = 0.75$, $h = 10$ mm; (d) $q = 0.17$; $h = 35$ mm; (e) $q = 1.6$, $h = 25$ mm. 1 mm and 3 mm glass beads appear respectively in blue and red and coriander grains in orange-yellow. (For interpretation of the references to color in this figure legend, the reader is referred to the web version of this article.)

For 1 mm glass beads, the angles θ corresponding to the 3 drop heights differ by up to 3° at early times, likely because the height of the pile is still small. The value of θ is particularly low (26.5°) for $h = 50$ mm, in this case, the kinetic energy of the impacting beads is sufficient to induce a flow of the whole pile: beads are carried away from the apex and the angle θ of the pile with the horizontal remains low. For the two other heights, instead, the beads remain closer to the impact point and the value of θ is significantly higher (28 and 29.5°).

At times $100 \lesssim t \lesssim 200$ s, the angles θ for different values of h differ generally by less than 0.3° and decrease slightly with time (by about 0.6°): the local height of the pile is large enough so that even fast grains obtained for $h = 50$ mm lose all their energy by interacting with the surface. In this regime, the angles θ_R and θ_M differ by less than 1° (Table 1). The transition between the two regimes takes place slightly later for $h = 50$ mm because there is more kinetic energy to dissipate.

For 3 mm glass beads and $h = 50$ mm, θ is low at early times ($\simeq 26°$) and increases thereafter ($t \gtrsim 100$ s) like for $d = 1$ mm. At long times, however, the dispersion of the values of *theta* measured for the different values of h is much larger than for $d = 1$ mm. For $t \gtrsim 120$ s, the mean value of θ is overall larger for $d = 3$ mm than $d = 1$ mm: more precisely, the value of θ_R is similar to that for $d = 1$ mm while θ_M is significantly larger (Table 1). Globally, these results are in agreement with those reported by previous authors [14,15]. The origin of these features is discussed at the end of the present section.

For coriander grains, the time necessary for reaching similar values of θ for the different drop heights increases to ~ 130 s. The amplitude of the subsequent variations of θ is similar to that measured for 3 mm glass beads while the values of the angle are overall larger: this time, both θ_M and θ_R are larger than for glass beads (Table 1). This difference likely reflects the influence of the roughness. The differences between the values of the angle θ for the 3 types of beads are visible in Fig. 2d in which all 3 curves correspond to a same drop height ($h = 30$ mm). As mentioned above, for $t \gtrsim 80$ s, the minimum values ($\simeq \theta_R$) are similar for the two diameters of glass beads while the maximum values ($\simeq \theta_M$) are larger for $d = 3$ mm.

The mechanisms determining the mean angle of the piles in the above experiments may be expected to be related to those controlling the motion of single beads over rough planes studied in such works as Refs. [16–18]: in both cases, the motion of the particles at the surface of the pile or the plane is indeed a key element. These latter studies put in evidence a transition from a deceleration to a constant velocity creeping motion and, then, to saltation as the tilt angle of the plane from horizontal increases. These transitions take place at lower angles when the relative roughness (ratio of the characteristic length of the roughness to the bead size) decreases; the angle is also lower when the roughness is created by small spherical glass beads rather than by sand grains with irregular shapes. Similarly, in the decelerated regime, the motion stops after a larger distance when the relative roughness decreases and, when the velocity is constant with time, it is larger for a low relative roughness. A similar transition from creeping to saltation may occur in the present process when the drop height (and, therefore the kinetic energy) increases from $h = 10$ to $h = 30$ or 50 mm. Then, large slopes may be expected to subsist for a longer time when there is no saltation: this would account for the large peak values of θ in Fig. 2b–c. Increasing friction would further increase the peak values of θ as is indeed the case for coriander grains.

3.2. Identification of the different mixing/segregation regimes

Fig. 3a–e displays the typical views of piles corresponding to different mixing/segregation regimes and obtained for different values of the control parameters q and h and different sets of grains.

Fig. 3a–b were obtained by building-up the heap from 1 mm glass beads (blue) and 3.1 mm coriander seeds (orange-yellow) which are less dense (see Section 2) and have a rougher surface than the beads. In case (a), one has a macroscopically uniform random distribution of the coriander seeds with a concentration gradually decreasing in the central part; no layers are observed. In the following, such distributions are said to correspond to a "mixing" regime (or *M*). In case (b), instead, the separation is complete: there are no coriander seeds in the central part (except right at the surface) and they are fully concentrated on the sides. Only a very weak onset of layering is visible in the middle of the left boundary between the large and small grains. Such configurations correspond to the "segregation regime" (or *S*).

Fig. 3c–e was obtained by using glass beads of same densities and same surface roughness but with diameters similar to those encountered in the previous case (1 and 3 mm). In Fig. 3c, a layered structure is clearly visible in a large fraction of the heap: this "layered regime" is designated by "*L*". In Fig. 3d and e, the identification of the flow regimes is not as clear as in the three previous cases. In case 3d, the small beads (blue) are essentially located in the center of the pile and the larger ones (red) in the aisles: however, layers are visible (particularly on the left side) at the boundary between the two regions. We shall refer to this regime as the *S–L* one. In case 3e, no layers are visible: the 1 mm beads are mostly grouped in the central part but a few of them are dispersed on the sides. Similarly, in the central part, some 3 mm beads are mixed with the 1 mm ones. One deals therefore with a case intermediate between the segregated and the mixed regimes which is referred to in

the following as *S–M*. These experiments have been repeated for a broad range of values of q and h.

Quantitatively, the mixing/segregation/layered regime is identified by comparing the spatial variations of two indices I_H and $I_\perp$ [10]: these correspond to the relative volume fraction of large particles in two sets of stripes, all of equal area, paving the image of the pile: I_H corresponds to vertical stripes while, for $I_\perp$, the stripes are parallel to the mean surface of the pile. The variation of I_H and $I_\perp$ is studied in the direction perpendicular to the corresponding stripes. For instance, I_H varies linearly with distance in the case of segregation but remains constant for both mixing and layering; in contrast, $I_\perp$ varies much more with the normal distance to the surface in the case of layering than for mixing or segregation. This analysis leads to the two maps of Fig. 4 corresponding respectively to experiments using coriander seeds (a) and 3 mm glass beads as the large particles.

For experiments using coriander seeds and smaller glass grains, one first notes that neither the layered nor the segregated-mixed regimes are observed even if q and/or h are varied (Fig. 3b). As h increases, one observes instead a direct transition from the segregation to the mixing regime: it is likely induced by the increased kinetic energy of the grains impinging on the pile. This influence of the kinetic energy on the granular dynamics is confirmed by the saltation of the grains moving down the slope which occurs for $h \geq 50$ mm. The transition between the segregation and mixing regimes takes place at a lower value of h when q increases. Finally, one notes that no large scale avalanches were observed for the coriander grains.

The above results differ very much from those obtained using 3 mm and 1 mm glass beads [10] and plotted in Fig. 4b. On the one hand, layering does occur in this case, but only for low ratios $q \lesssim 2$: it is particularly developed for smaller drop heights ($h \lesssim 30$ mm). On the other hand, the mixing regime is only observed for the largest values of h and q. For $h > 30$ mm, like in Fig. 3d, the packings are largely segregated but layers may be visible locally (*S–L* regime). For higher ratios q, like in Fig. 3e, one observes the segregation mixing regime (*S–M*) with two separate regions in which both species remain present but with different relative concentrations.

The above comparison shows that segregation is enhanced by replacing the 3 mm glass beads by coriander ones of similar diameter: both the higher density difference between the large and small grains (reducing the kinetic energy of the large ones) and the rougher surface of the coriander grains may account for this result.

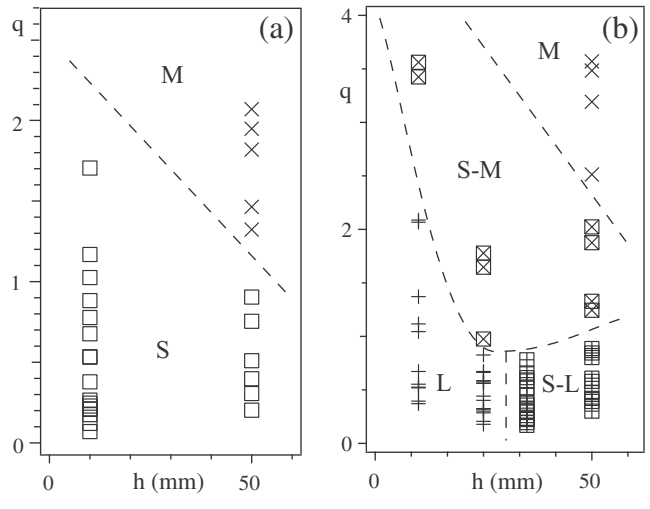

Fig. 4. Maps of the mixing regimes observed as a function of the drop height h and of the ratio q of the volume flow rates; in both maps, the gray lines between the different regimes are just aids for the eye : (a) $d_1 = 3.1$ mm (coriander), $d_2 = 1$ mm (glass), (b): $d_1 = 3$ mm (glass), $d_2 = 1$ mm (glass). Symbols corresponding to the different flow regimes — (+): layered (*L*); (×): mixed (*M*); (□): segregated (*S*); (⊞): segregated–layered (*S–L*); (⊠): segregated–mixed (*S–M*).
Graph (b) includes data from Ref. [10] shown for comparison.

3.3. Time variation of the tilt angle of the free surface of mixtures of grains of different sizes

The variation with time of the mean angle of the surface of the pile to the horizontal provides important information on the dynamics of the process, particularly regarding the occurrence of avalanches and the relative fraction of small and large grains near the surface.

For coriander grains and 1 mm glass beads, after an initial transition regime, the variation of θ with time is smooth and very similar for two pairs of values of q and h corresponding to the segregation and mixing regimes. The difference between θ_R and θ_M is also smaller ($\sim 1°$) than for coriander grains only. These curves resemble those obtained using only 1 mm glass beads, rather than only coriander grains (Fig. 2). The value of θ is however closer to that corresponding to the latter (θ_{R1}); moreover, the concentration of coriander grains near the surface is high (Fig. 3a–b). Adding small beads to the coriander grains appears to make their motion easier and to reduce blockage or trapping effects: in the analogy with the motion of a grain over a rough plane (Section 3.1), the addition of small beads may be equivalent to reduce the roughness of the plane.

For mixtures of 1 and 3 mm glass beads, the time variation of θ depends significantly on the regime. Fig. 6a displays the variation in the layered regime: θ slowly increases up to a maximum value $\theta_M \simeq 34°$ and then falls rapidly during and after a large avalanche before starting to increase again. The above value is close to the maximum angle of stability θ_{M1} for large beads (Table 1). The angle after the avalanche is approximately the angle of repose θ_{R2} for small beads. Then, θ keeps decreasing down to a minimum value $\theta_m \simeq 25°$ significantly lower than all those measured with a single type of grains.

In order to analyze this result, we performed complementary experiments using a downflow of 3 mm glass beads over a pile of smaller 1 mm ones and for a same drop height $h = 10$ mm (Fig. 6b). In this case, starting from the angle of repose θ_R, θ decreases quickly down to a lower minimum $\theta_m \simeq 25°$ like in the layered regime before rising slower again. This suggests that the variation of θ in Fig. 6a–b reflects the interaction of the large beads with a layer of small ones.

The pictures of Fig. 7 illustrate this behavior: they correspond to times t_{1-4} in Fig. 6a. At $t = t_1$ (Fig. 7a), the pile is almost completely covered by a layer of large beads with an upper boundary (arrow) acting as a barrier blocking the motion of the smaller ones. In this phase, the angle θ corresponds to that for a pile of large beads: an avalanche occurs

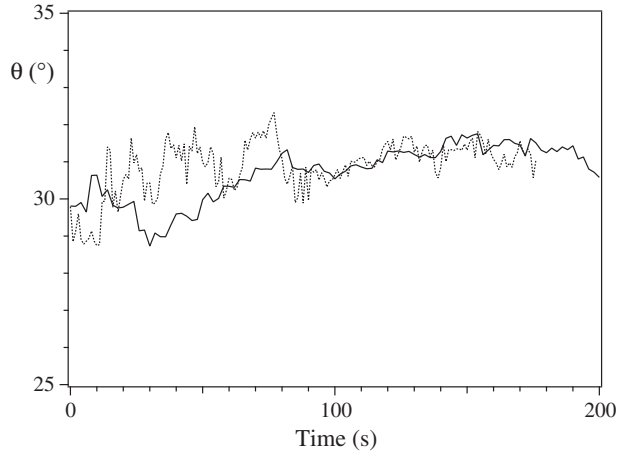

Fig. 5. Variation with time of the mean angle θ of the surface with the horizontal during the build-up of a pile of mixed coriander grains ($d_1 = 3.1$ mm) and glass beads ($d_2 = 1$ mm). Continuous line: $q = 0.9$, $h = 10$ mm (segregation); dotted line: $q = 1.95$, $h = 50$ mm (mixing). Time interval between data points on the curves: 1 s (30 frames).

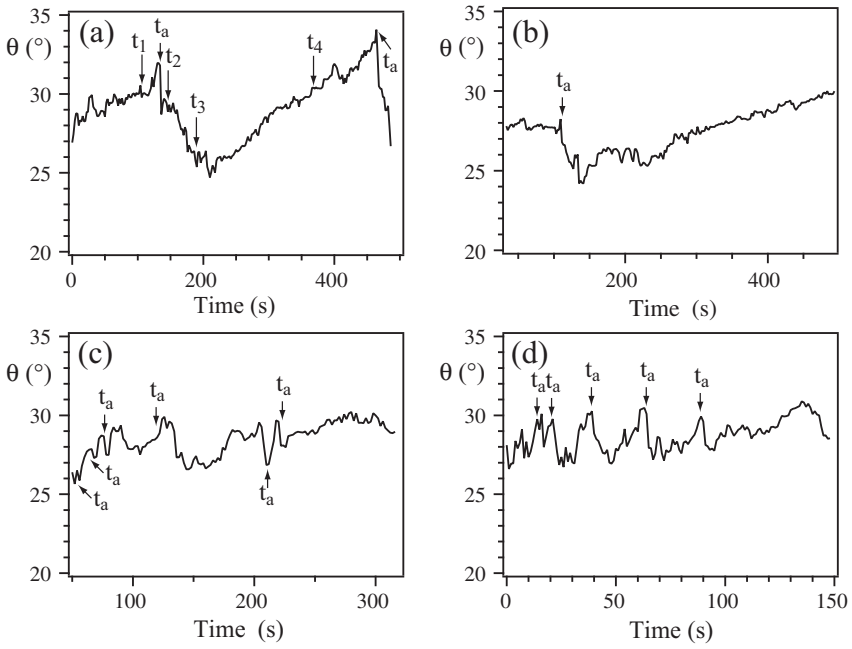

Fig. 6. Variation of the mean angle θ during the build-up of a pile of mixed glass beads of diameters $d = 1$ mm and $d = 3$ mm. Time interval between data points: 1 s (30 frames); arrows marked t_a correspond to the onset of avalanches. a) $q = 0.83$, $h = 10$ mm (layering); times t_1, t_2, t_3 and t_4 correspond to the pictures of Fig. 7; $t_a = 132$ and 464 s. b) Slope angle variation for 3 mm glass beads falling over a pile of 1 mm beads ($h = 10$ mm); $t_a = 109$ s. c) $q = 2.5$, $h = 50$ mm (mixing); $t_a = 54$, 66, 80, 124, 186 and 223 s. d) : $q = 1.5$, $h = 50$ mm (segregation–mixing); $t_a = 14$, 22 , 39, 63 and 90 s.

(t_a) when θ reaches the corresponding maximum angle of stability θ_{M2}. The avalanche carries away the large beads and leaves, at the time t_2 (Fig. 7b), a layer of flowing small beads with θ close to the angle of repose θ_{R1}. Large beads flow above this layer (Fig. 7c) and gather at the bottom of the pile (d of the figure). Finally, a new layer of large beads builds up on the pile, starting from the bottom with its boundary rising on the slope (Fig. 7d) and θ rises again. The curve of Fig. 6 would correspond to a similar process, starting at time t_2 instead of time t_1. The disappearance of the layered regime above a value of q decreasing at larger heights h may reflect a lack of blockage of the flow of large grains when the corresponding flow rate and, therefore, q becomes too large. Fig. 6c displays the time variation of θ in the mixing regime which is only observed for the largest drop height ($h = 50$ mm) and for large ratios q (2.5 in Fig. 4b). The amplitude of the variations of θ is significantly smaller than in the layered regime. This amplitude is of the same order of magnitude as for only 3 mm beads but the extremal values $\theta_M \simeq 30°$ and $\theta_m \simeq 27°$ are lower (see Table 1 and Fig. 2b); θ_M and θ_m are also lower than for the mixture of coriander grains and 1 mm beads.

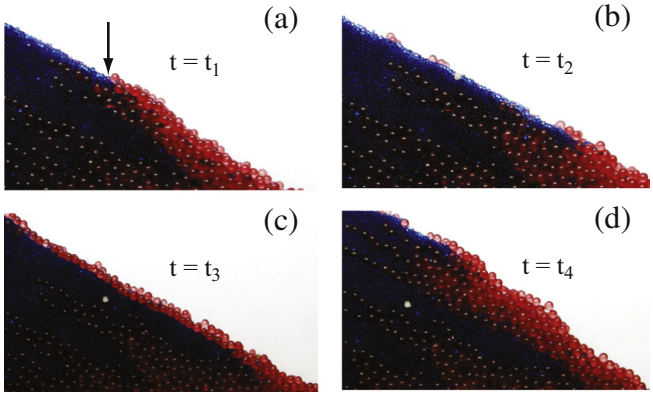

Fig. 7. Views of the pile in the layered regime of Fig. 6a at times $t_1 = 105$ s (a), $t_2 = 140$ s (b), $t_3 = 188$ s (c), $t_4 = 364$ s (d) (field of view 140×90 mm).

In the intermediate segregation–mixing (*SM*) regime, still for $h = 50$ mm but for $q = 1.5$, the variation of θ is approximately cyclical during the first half of the recording. The minimum and maximal angles are of the same order (to within $\pm 0.5°$) as in the mixing regime. In these regimes, the magnitude of the avalanches is much smaller than in the layering regime (Fig. 6a).

The variations of θ with time displayed in Figs. 6 and 5 for mixtures of two different species differ strongly from those corresponding to a single species of grains (Fig. 2). The variability of the angle over short periods of time is lower than for large glass beads or coriander grains and of the same order of magnitude as for small glass beads: this may indicate that, for instance, the motion of large grains is made easier by the appearance of layers of smaller beads (like for a smooth plane, as discussed at the end of Section 3.1). In contrast the longer term variability of θ is larger, particularly at long times due to the occurrence of processes like avalanches involving a large number of grains.

3.4. Spatiotemporal diagrams — evaluation of grain or bead velocities

While the variations of θ with time correspond to the large scale deformations of the pile and depend on the mixing/segregation regime, spatiotemporal diagrams show the motion of individual (or groups of) grains and provide information on local processes. These diagrams (Figs. 8 and 9) display as gray levels vertical local displacements Δz of the surface of the pile between two subsequent frames (grayscale) as a function of time and of the horizontal distance x. A single grain moving along the surface appears, for instance, as two closely spaced parallel lines, one lighter and one darker than the background gray level (lines marked 2 in Fig. 8a): these lines mark the times at which the bead enters (resp. leaves) the corresponding pixel so that the local height $z(x, t)$ of the surface of the pile increases (resp. decreases).

Practically, only the motion of large beads or grains (or groups of them) is visible on the diagram: variations of the local height due to the motion of a small 1 mm glass bead are too small to be detectable. The fast motion by saltation of large or small beads at a distance above the surface does not influence the surface profile is not detected either. The velocity of these displacements is determined from the slope

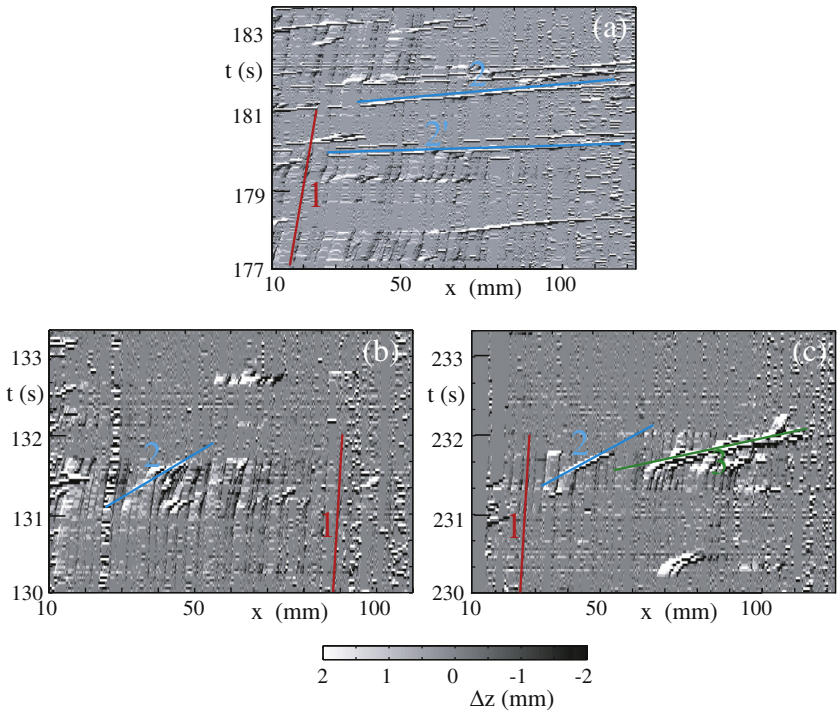

Fig. 8. Spatiotemporal diagrams of the motion of coriander seeds ($d_1 = 3.1$ mm) during the flow of a mixture of these grains with 1 mm glass beads in the segregated regime ($q = 0.8$, $h = 10$ mm). Vertical scale: time; horizontal scale: distance along the x axis ($x = 0$: apex of the pile). Grayscale: variation $\Delta z(x, t)$ of the local height $z(x)$ of the surface during the time lapse $\delta t = 1/30$ s (scale at the bottom center). Diagrams correspond to a small fraction of the total recording time (time scales at the left). Apex of the pile located outside the diagram, at ~ 10 mm from the left boundary. (a) Motion of individual coriander seeds over layers of the same seeds covering a packing of smaller glass beads ($d_2 = 1$ mm) in the segregated regime. (b) Motion of a patch of seeds; (c) local avalanche.

of the corresponding spatiotemporal "trajectories": quantitatively, it is proportional to the ratio $\Delta n_p/\Delta n_f$ in which Δn_p is the number of pixels along x between two points of the trajectory in the diagram and Δn_f is the corresponding number of frames between these two same points. In order to obtain values of the velocity in mm/s, t $\Delta n_p/\Delta n_f$ is multiplied by 30/8 = 3.75 (time interval between two frames: 1/30 s, (distance

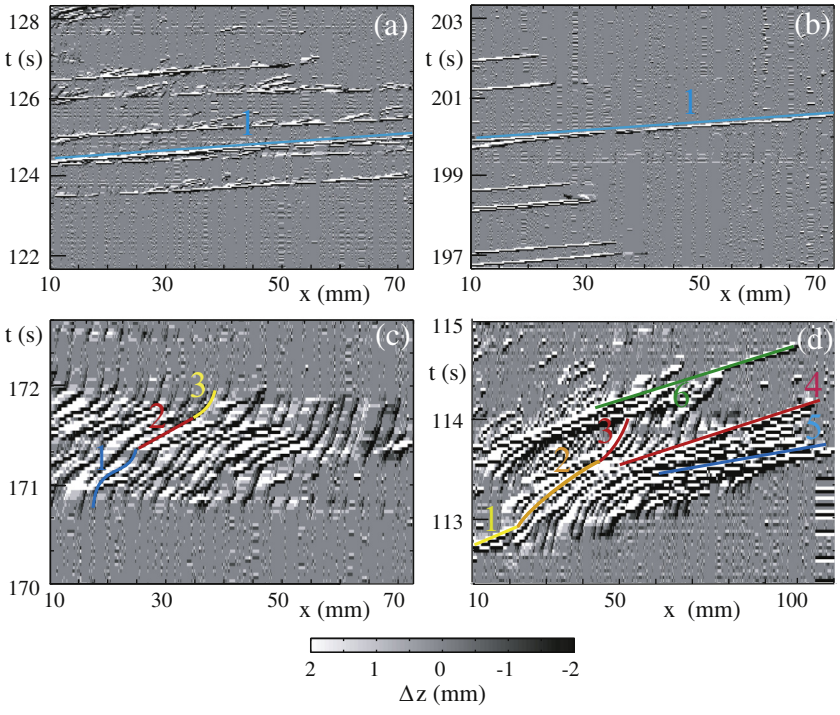

Fig. 9. Spatiotemporal diagrams obtained like those of Fig. 8 for a mixture of glass beads of sizes ($d_1 = 3$ mm and $d_2 = 1$ mm) in the layered regime ($q = 0.83$, $h = 10$ mm) – (a–b): individual 3 mm beads moving over (a) a pile of 1 mm beads, (b) over a continuous cap of 3 mm beads laid over a similar pile. (c) Motion of a patch of 3 mm beads (d) avalanche event involving 3 mm beads.

between pixels along x: 1/8 mm). The range of velocities of the different types of grain displacements displayed in the diagrams is listed in Table 2.

Fig. 8a–c was obtained in the segregation regime using a mixture of coriander grains and 1 mm glass beads. Events similar to those displayed in this figure are also observed in the mixing regime. Fig. 8a corresponds to the motion of a few individual coriander grains over a layer of the same grains. The path length is in the order of the size of the pile; the velocities remain generally constant during the displacements with a broad range of values up to 250 mm · s^{-1} (see #2). The dark, parallel, near vertical lines correspond to a global slow motion of the cap of coriander grains closest the surface (velocity ~ 2 mm · s^{-1} for the red line # 1).

A similar slow motion is visible at early times in Fig. 8b (line 1) and accelerates between $t = 131$ and 131.5 s before stopping: during this time lapse, a few grains move by 3 grain diameters or so at larger velocities (≃ 45 mm · s^{-1} for line #2). Both types of motions also appear in Fig. 8c (lines # 1 and # 2) with velocities of the same order of magnitude. Small scale avalanches (line # 3) with a larger path length (> 10 d) and velocity (≃ 105 mm · s^{-1}) are also visible: only a few grains are involved, unlike for large scale avalanches which are only observed for mixtures of glass beads (see below).

The diagrams of Fig. 9c–d correspond to 3 and 1 mm glass beads in the layered regime. Most features reported below (except large avalanches) are however also observed in the segregation and mixing regimes.

The key difference with coriander grains is the occurrence of large avalanches observed only for glass beads: a reason may be the kinetic energy of the coriander grains which is too small to overcome the friction forces and, therefore, to trigger the avalanches. Fig. 9e displays an avalanche triggered by the impact of two large beads moving rapidly down the slope from the top of the pile (line # 1 in the graph): they transfer their momentum to a group of large beads and accelerate them (~ 40 mm · s^{-1} for line # 2). Some of these beads slow down after moving down about half of the slope (line # 3) while others move all the way to the bottom (even though they may briefly stop on the way). As deduced from the different slopes of the lines, the velocities of the corresponding beads are different (~ 80 and 150 mm · s^{-1} for lines # 4 and # 5) and the fastest ones overtake other, slower, beads. These avalanches move along a large fraction of the width of the piles. There remains a surface of 1 mm beads cleared of 3 mm ones so that isolated beads move easily like in Fig. 9a: new beads injected at the top of the pile move then all the way down to the bottom (~ 80 mm · s^{-1} for line #6).

Overall motions of smaller groups of 3 mm beads were also observed (Fig. 9c): three different phases of the motion are marked as # 1, # 2 and # 3 and correspond respectively to an acceleration (downward curvature), a constant velocity phase (straight part) and a deceleration one (upward curvature). The maximum velocity in the stationary phase (~ 50 mm · s^{-1}) is smaller than for individual beads (Table 2): this may be due to stronger friction and to the loss of energy during inelastic collisions. Here, both the number of grains involved and the path length are generally larger than for coriander grains: this may reflect a friction of the smooth glass beads with the underlying layers and the surrounding beads weaker than for rough coriander grains.

Fig. 9a and b displays the downward motion of individual 3 mm glass beads (oblique lines in the diagrams) respectively at the surface of a packing of 1 mm beads or above a layer of 3 mm beads laid over such a packing. Both the path length and the velocity are of the same order of magnitude as for coriander grains.

Unlike for coriander grains, we did not observe a slow global motion of layers of large glass beads. This may be due to the weaker friction between glass beads than between coriander grains which makes their relative displacements easier: unlike coriander grains, glass beads do not then move as a block but independently.

Table 2
Typical velocities of the different types of motions of the coriander grains and 3 mm glass beads. The ranges of values listed in the table correspond to different experiments performed in different flow regimes.

Type of bead/grain motion	Range of velocities [mm/s]
- Individual 3 mm glass beads moving over a layer of 3 mm glass beads:	100–250
- Individual 3 mm glass beads moving over a layer of 1 mm glass beads:	100–250
- Individual 3.1 mm coriander grains moving over a layer of coriander grains:	100–250
- Slow global motion of a layer of coriander grains	1–5
Motion of patches of 3 mm glass beads:	40–60
- Motion of patches of coriander grains (layered regime):	40–60
- Avalanches of 3 mm glass beads in the layered regime:	75–125

4. Conclusion

The present experiments have shown that piles with a layered structure may be created from a mixture of smooth grains of same spherical shape and same density but of different sizes. The difference between the sizes is in this case sufficient to induce the layering. This differs from the observations of other authors suggesting that a difference between the roughness of the grains and their individual geometry was a mandatory ingredient of layering. Moreover, replacing the large glass beads by lighter and rougher coriander ones of same size eliminates the layered regime instead of enhancing it. Moreover, there is always some amount of mixing in the case of glass beads of two sizes while complete segregation was observed only when the large grains are coriander seeds.

The layering regime is shown to be associated to large scale avalanches involving a large number of grains and propagating over distances of the order of the width of the piles; such large avalanches were not observed in the segregation and mixing regimes. Spatiotemporal diagrams of the surface of the pile show that these avalanches are triggered by the impact of fast moving grains on steps and/or wedges acting as obstacles blocking the motion of grains located upstream of them. An important consequence of these large avalanches is the large amplitude of the variations of the slope of the piles with time which is an important characteristic of the layered regime.

For mixtures of coriander grains and small glass beads, only small-scale avalanche-like motions of patches of a few grains are observed: this is in agreement with the lack of layered regime for mixtures using these grains. This important difference is likely due to the higher friction and lower kinetic energy of the coriander grains.

Moreover, spatiotemporal diagrams allowed us to detect slow global motions of the upper layer of coriander grains: the motion of a small number of these grains may accelerate locally. When coriander seeds are replaced by glass beads as the large grains, these slow global motions are not observed and are replaced by either faster displacements of a larger number of grains or by avalanches.

Globally, the different shapes, densities and roughness of the glass beads and coriander seeds influence very much the flow and mixing regimes: in the first case, layers (and avalanches) frequently appear and in the second, the segregation may be more complete. For a same flow regime, the range of velocities is similar for the two sets of grains.

The results of the present study point towards several issues which will have to be studied in future work: a first one is to attempt to separate the effects of the roughness and the density on the observations by using lighter smooth round beads like hollow glass beads or plastic beads although, in the latter case, the restitution coefficient may be different. It will also be necessary to investigate the magnitude of the wall effects by varying the gap e of the cell in order to determine its influence on the velocity of the grains and the occurrence of avalanches. The dependence of these parameters on the ratio d_1/d_2 is also an important

issue since experiments reported in Ref. [10] did not report layering for $d_1/d_2 = 3/2$. An important feature is the reduced short variability of the mean angle of piles of mixtures of large and small grains compared to piles containing only large grains: this should be investigated for variable relative flow rates of small grains. In a later stage, one should attempt to extend these results to three-dimensional piles: it is indeed not clear that the mechanisms leading to layering in *2D* systems may take place in a coherent manner in all radial directions of a *3D* pile. During the build-up of *3D* piles from mixtures of grains it will therefore be important to look for large scale avalanches at their surface and determine the dependence of their duration and width on the characteristics of the grains and of the flowing mixture.

Acknowledgments

We acknowledge the support of the LIA PMF-FMF (Franco-Argentinian International Associated Laboratory in the Physics and Mechanics of Fluids), of PIP CONICET 1022 and of project UBACYT 20020100100899.

References

[1] H.A. Makse, S. Havlin, P.R. King, H.E. Stanley, Spontaneous stratification in granular mixtures, Nature 386 (1997) 379–381.
[2] H.A. Makse, P. Cizeau, H.E. Stanley, Possible stratification mechanism in granular mixtures, Phys. Rev. Lett. 78 (1997) 3298–3301.
[3] H.A. Makse, Stratification instability in granular flows, Phys. Rev. E. 56 (1997) 7008–7016.
[4] B. Urbanc, L. Cruz, Order parameter and segregated phases in a sandpile model with two particle sizes, Phys. Rev. E. 56 (1997) 1571–1579.
[5] H.A. Makse, P. Cizeau, H.E. Stanley, Modeling stratification in two-dimensional sandpiles, Phys. A Stat. Mech. Appli. 249 (1998) 391–396.
[6] H.A. Makse, R.C. Ball, H.E. Stanley, S. Warr, Dynamics of granular stratification, Phys. Rev. E. 58 (1998) 3357–3367.
[7] Y. Grasselli, H.J. Herrmann, Experimental study of granular stratification, Granul. Matter 1 (1998) 43–47.
[8] P. Cizeau, H.A. Makse, H.E. Stanley, Mechanisms of granular spontaneous stratification and segregation in two-dimensional silos, Phys. Rev. E. 59 (1999) 4408–4421.
[9] N. Vandewalle, Phase segregation and avalanches in multispecies sandpiles, Phys. A 272 (1999) 450–458.
[10] J.G. Benito, I. Ippolito, A.M. Vidales, Novel aspects on the segregation in quasi 2D piles, Powder Technol. 234 (2013) 123–131.
[11] L. Bruno, A. Calvo, I. Ippolito, Dispersive flow of disks through a two-dimensional Galton board, Eur. Phys. J. E: Soft Matter 11 (2003) 131–140.
[12] J.G. Benito, I. Ippolito, A.M. Vidales, Improving mixture of grains quality using bidimensional Galton boards, Phys. A 387 (2008) 5371–5380.
[13] S. Balasubramanian, K.K. Singh, R. Kumar, Physical properties of coriander seeds at different moisture content, Int. Agrophys. 26 (2012) 419–422.
[14] C.M. Dury, G.H. Ristow, J.L. Moss, M. Nakagawa, Boundary effects on the angle of repose in rotating cylinders, Phys. Rev. E. 57 (1998) 4491–4497.
[15] X.Y. Liua, E. Spechta, J. Mellmann, Experimental study of the lower and upper angles of repose of granular materials in rotating drums, Powder Technol. 154 (2005) 125–131.
[16] M.A. Aguirre, I. Ippolito, A. Calvo, C. Henrique, D. Bideau, Effects of geometry on the characteristics of the motion of a particle rolling down a rough surface, Powder Technol. 92 (1997) 75–80.
[17] C. Henrique, M.A. Aguirre, A. Calvo, I. Ippolito, S. Dippel, G.G. Batrouni, D. Bideau, Energy dissipation and trapping of particles moving on a rough surface, Phys. Rev. E. 57 (1998) 4743–4750.
[18] L. Samson, I. Ippolito, D. Bideau, G.G. Batrouni, Motion of grains down a bumpy surface, Chaos 9 (1999) 639–648.
[19] Y. Fan, Y. Boukerkour, T. Blanc, P.B. Umbanhowar, J.M. Ottino, R.M. Lueptow, Stratification, segregation, and mixing of granular materials in quasi-two-dimensional bounded heaps, Phys. Rev. E. 86 (2012) 051305.
[20] J.P. Koeppe, M. Enz, J. Kakalios, Phase diagram for avalanche stratification of granular media, Phys. Rev. E. 58 (1998) R4104.